Title:

Zinc supports transcription and improves meiotic competence of growing bovine oocytes

Valentina Lodde[1]*, Rodrigo Garcia Barros[1], Priscila Chediek Dall'Acqua[2,3], Cecilia Dieci[1], Claude Robert[4], Alexandre Bastien[4], Marc-André Sirard[4], Federica Franciosi[1] and Alberto Maria Luciano[1]

[1]Reproductive and Developmental Biology Laboratory (Redbiolab), Department of Health, Animal Science and Food Safety "Carlo Cantoni", Università degli Studi di MIlano, 20133 Milan, Italy; [2]Department of Preventive Medicine and Animal Reproduction, School of Agricultural and Veterinarian Sciences, São Paulo State University (UNESP), Jaboticabal, Brazil; [3]Laboratory of Reproductive Physiology, School of Veterinary Medicine, São Paulo State University (UNESP), Araçatuba, Brazil; [4] Centre de Recherche en Reproduction, Développement et Santé Intergénérationnelle (CRDSI), Département des Sciences Animales, Université Laval, Québec, Canada, G1V 0A6

Corresponding Author: Valentina Lodde, Dipartimento di Scienze Veterinarie per la Salute, la Produzione Animale e la Sicurezza Alimentare, Università degli Studi di Milano, Via Celoria, 10 - 20133 Milano, Italy - Phone (+39) 02 50317978 - valentina.lodde@unimi.it

Short Title:

Zinc in bovine growing oocytes

Key Words A minimum of four keywords describing the manuscript

Oogenesis, meiosis, oocyte competence, cumulus cells, transcription, chromatin, zinc transporters, ZIP, Znt metallothionein, SLC39A, SLC30A, DNA methylation

Word count of the full article: 6059

Abstract

In the last years many studies focused on the understanding of the possible role of zinc in the control of mammalian oogenesis, mainly on oocyte maturation and fertilization. However, little is known about the role of zinc at earlier stages, when the growing oocyte is actively transcribing molecules that will regulate and sustain subsequent stages of oocyte and embryonic development. In this study we used the bovine model to gain insights into the possible involvement of zinc in oocyte development. We first mined the EmbryoGENE transcriptomic dataset, which revealed that several zinc transporters and methallothionein are impacted by physiological conditions throughout the final phase of oocyte growth and differentiation. We then observed that zinc supplementation during in vitro culture of growing oocytes is beneficial to the acquisition of meiotic competence when subsequently subjected to standard in vitro maturation. Furthermore, we tested the hypothesis that zinc supplementation might support transcription in growing oocytes. This hypothesis was indirectly confirmed by the experimental evidence that the content of labile zinc in the oocyte decreases when a major drop in transcription occurs in vivo. Accordingly, we observed that zinc sequestration with a zinc chelator rapidly reduced global transcription in growing oocytes, which was reversed by zinc supplementation in the culture medium. Finally, zinc supplementation impacted the chromatin state by reducing the level of global DNA methylation, which is consistent with the increased transcription. In conclusion our study suggests that altering zinc availability by culture medium supplementation supports global transcription, ultimately enhancing meiotic competence.

Introduction

From the time zinc was discovered to be the most abundant transition metal in mouse oocytes (Kim et al., 2010), many studies have focused on the understanding of its possible role in the control of mammalian oogenesis. Thus far, most of the studies considered the function of zinc during oocyte maturation and fertilization. These studies seem to indicate that zinc regulates distinct molecular mechanisms during the two stages, in line with the notion that zinc participates in a vast number of biological processes (Maret, 2017).

In the immature fully grown oocyte, zinc is implicated in the maintenance of meiotic arrest (Kong et al., 2012, Tian and Diaz, 2012). Conversely, during maturation, there is a rise in total zinc content, which is key for successful oocyte maturation (Kim et al., 2010, Bernhardt et al., 2011, Tian and Diaz, 2012, Kong et al., 2014, Jeon et al., 2015). In the MII stage oocyte the quota of zinc loosely bound to biomolecules in a readily exchangeable form (Outten and O'Halloran, 2001, Dean et al., 2012), referred to as “labile zinc” or “free zinc”, is accumulated in cortical vesicle-like structures that are released in the extracellular compartment upon fertilization through repetitive exocytic events termed “zinc sparks”, which are in turn implicated in the process of meiotic resumption and block of polyspermy (Bernhardt et al., 2012, Duncan et al., 2016, Kim et al., 2011, Que et al., 2015, Que et al., 2017, Que et al., 2019, Zhao et al., 2014). The molecular mechanisms by which zinc regulates all these processes are just starting to be elucidated. However, in reason of the global transcriptional silencing in the fully-grown oocytes, they must be transcription-independent.

To date, less is known about the role of zinc at earlier stages of oocyte development, i.e. during oocyte growth, when these cells are actively transcribing molecules that will regulate and sustain subsequent stages of oocyte and early embryonic development. The first indication that zinc is fundamental during oocyte growth comes from in vivo studies in the mouse.

Specifically, it has been shown that a zinc-restricted diet 3–5 days before ovulation disrupts oocyte maturation as well as embryonic, fetal and placental development at various levels (Tian et al., 2014, Tian and Diaz, 2012, Tian and Diaz, 2013). Moreover, studies in mouse growing oocytes with uncondensed chromatin in the Non Surrounded Nucleolus (NSN) configuration, have shown that zinc modulation regulates the localization of the metal response element-binding transcription factor-1 (MTF-1) (Kong et al., 2014), which is a well characterized transcription factor that functions as a cellular zinc sensor by coordinating the expression of genes involved in zinc homeostasis (Andrews, 2001).

To further advance the knowledge on the role of zinc during oogenesis, we propose the bovine as experimental model since the changes that occurs within the nucleus during the latest phases of oocyte growth and differentiation before meiotic resumption have been well characterized (reviewed in (Luciano and Lodde, 2013, Luciano et al., 2014b, Bogolyubov, 2018). In cattle, as in other mammals, changes in large-scale chromatin configuration in the Germinal Vesicle (GV) are used as a morphological marker of oocyte differentiation (De La Fuente, 2006, Zuccotti et al., 2005, Luciano et al., 2014a, Luciano and Lodde, 2013, Bogolyubov, 2018). Specifically, four stages of GV oocytes, from GV0 to GV3, have been characterized by increasing level of chromatin compaction (Lodde et al., 2007, Lodde et al., 2008, Lodde et al., 2009). GV0 oocytes, which typically show uncondensed chromatin, represent the high majority (around 80%) of oocytes collected from early antral follicles (0.5–2 mm), are still growing, meiotically non-competent, transcriptionally active and display low levels of global DNA methylation. In contrast, oocytes with increasing levels of compaction (GV1, GV2 and GV3) are considered “fully grown” and are typically collected from medium antral follicles, 2-8 mm in diameter. GV1, GV2, and GV3 oocytes are meiotically competent, while they differ in the ability to form blastocyst after in vitro fertilization, with GV1 oocytes being less competent than GV2 and GV3. Notably, a major drop in transcription occurs during

the transition from GV0 to GV1 configuration, similar to the mouse non-surrounded nucleolus/surrounded nucleolus (NSN/SN) transition, also described in humans and other mammalian species (reviewed in (Luciano and Lodde, 2013). GV0 to GV1 transition also entails increased levels of global DNA methylation (Lodde et al., 2009).

The bovine model offers the additional following advantages for the purpose of the proposed study. Firstly, a system for the In Vitro Culture of Oocyte, termed IVCO, is available in cattle (Luciano et al., 2011). Thanks to the use of physiological doses of FSH and PDE3 inhibitors, this system is able to promote the crosstalk between oocytes and cumulus cells and in turn the oocyte growth and the increase of their meiotic competence of when they are further subjected to standard in vitro maturation (IVM) condition (Luciano et al., 2011). Secondly, the transcriptomic profiles of bovine oocytes and surrounding cumulus cells at different stages of differentiation are available. Specifically they were assessed by microarray analysis (Labrecque et al., 2016, Labrecque et al., 2015, Dieci et al., 2016) within the EmbryoGENE program (http://emb-bioinfo.fsaa.ulaval.ca/Home/index.html), that has been implemented by collecting and storing transcriptomic data of bovine oocytes, cumulus and granulosa cells under different physiological conditions using the same transcriptomic platform and bioinformatic tools. After being analyzed and validated individually in their respective publication, all the collected transcriptomic data sets were subjected to meta-analysis as described in (Khan et al., 2016) and made publicly available through an interactive web interface called EmbryoGENE profiler, which thus provides dynamic expression profiles of any gene of interest in the selected sample (http://emb-bioinfo.fsaa.ulaval.ca/IMAGE/index.html).

Given the above observation, we have used the bovine growing oocyte as experimental model to assess the extent to which zinc plays a role during the latest phase of oocyte growth and differentiation and particularly to the hypothesis that zinc participates in the control of transcription at this stage.

Materials and methods

All chemicals and reagents were purchased from Sigma-Aldrich S.r.l. (Milan, Italy), unless otherwise stated.

EmbryoGENE dataset mining

The expression profile of genes encoding for proteins involved in intracellular zinc homeostasis (Kimura and Kambe, 2016) was assessed by mining the publicly available EmbryoGENE Profiler (http://emb-bioinfo.fsaa.ulaval.ca/IMAGE/index.html), which contains profiles of microarray expression data from a variety of tissues and conditions, collected by the researchers within the EmbryoGENE Network (http://emb-bioinfo.fsaa.ulaval.ca (Khan et al., 2016)). Specifically, the EmbryoGENE Profiler was mined to assess the expression profiles of: 1) members of the Solute Carrier Family 39 A (SLC39A), which encode for Zrt- and Irt-like Proteins (ZIP); 2) members of the Solute Carrier Family 30 A (SLC30A), which encode for Zn Transporters (ZnT) and 3) members of the protein coding gene Metallothioneins (MT). Three sets of previously published microarray data that cover the period of oocyte growth and acquisition of meiotic and developmental competence, were considered: 1) GEO series accession number GSE48283:oocytes collected from follicle of different size (<3, 3-5, >5-8, and >8 mm)(Labrecque et al., 2016); 2) GEO series accession number GSE48376: oocytes with different degree of chromatin compaction (GV0, GV1, GV2 and GV3) (Labrecque et al., 2015) and 3) GEO series accession number GSE79886; cumulus cells isolated from oocytes with different degrees of chromatin compaction (GV0, GV1, GV2 and GV3) (Dieci et al., 2016).

Importantly, each data set was validated by quantitative PCR as reported in each respective publication.

Oocytes collection and culture

Cumulus-oocytes complexes (COC) were collected and cultured as previously described (Lodde et al., 2007, Luciano et al., 2011). Briefly, bovine (Holstein Friesians) ovaries were harvested at a local abattoir (IT 2270M CE; Inalca S.p.A., Ospedaletto Lodigiano, LO, Italy) from pubertal females subjected to routine veterinary inspection and in accordance to the specific health requirements stated in Council Directive 89/556/ECC and subsequent modifications. The ovaries were transported to the laboratory within 2 hours in sterile saline solution maintained at 26°C. All the subsequent procedures, unless otherwise specified, were performed between 35°C and 38°C. COCs were retrieved from 2 to 8 mm middle antral follicles with a 19-gauge needle connected to an aspiration pump (COOK-IVF, Brisbane QLD, Australia) with a vacuum pressure of -28 mm/Hg. After aspiration, small pieces of ovarian cortex were sliced and examined under a dissecting microscope. COCs were isolated from early antral follicles (0.5 – 2 mm diameter) by rupturing the follicle wall with a 21-gauge needle. COCs were washed in Medium 199 supplemented with HEPES 20 mM, 1,790 units/L Heparin and 0.4% of bovine serum albumin (M199-D) and examined under a stereomicroscope. COCs from early antral follicles were collected within 2 hours. Only compact COCs with five or more complete layers of cumulus cells and a finely granulated homogenous ooplasm were used. The population of oocytes collected from this follicular class typically contain around 80% of GV0 stage oocytes and their mean diameter is 110 µm (Lodde et al., 2007, Luciano et al., 2011).

The in vitro culture of growing oocyte (IVCO) was performed as previously described with minor modification (Luciano et al., 2011). Oocytes were always cultured in the presence of cumulus cells as COCs. COCs were cultured in 500 µl of Medium 199 with 25 mM NaHCO3,

and further supplemented with 0.4% fatty acid free BSA, 0.68 mM L-glutamine, 0.2 mM sodium pyruvate, 0.1 mM cysteamine, 50 µg/ml of kanamycin, 10^{-4} IU/ml of recombinant human follicle-stimulating hormone (r-hFSH; Gonal F; Serono S.p.A.) and 10 µM cilostamide, for 24 h or for different times intervals according to the experimental design (see below), in four-well dishes (Nunc, Thermo Fisher Scientific, Waltham, MA, USA) at 38.5°C under 5% CO_2 in humidified air. According to the experimental design, IVCO medium was supplemented with 6.6 µg/mL zinc sulphate, which corresponds to 1.5 µg/µl of Zn^{2+}. This concentration is within the range of follicular fluid content and has been proved to be beneficial during bovine in vitro maturation (Picco et al., 2010, Anchordoquy et al., 2014). In a preliminary set of experiments, the IVCO medium was supplemented with 10 µM *N*,*N*,*N*′,*N*′-tetrakis (2-pyridinylmethyl)-1,2-ethanediamine (TPEN), a cell permeable zinc chelator (Kim et al., 2010). To assess the effect of zinc modulation on meiotic competence, after IVCO, COCs were washed in M199-D and cultured for 24h under standard serum free IVM conditions. IVM medium was M199 supplemented with 0.68 mM L-glutamine, 25 mM NaHCO3, 0.4% fatty acid-free BSA, 0.2 mM sodium pyruvate, 0.1 mM cysteamine, 50 µg/ml of kanamycin, and 0.1 IU/ml of r-hFSH (Luciano et al., 2011). To assess meiotic progression, at the end of IVM, cumulus cells were mechanically removed and oocytes were fixed in 4% paraformaldehyde in PBS for 30 min at room temperature, stained with DAPI, and analyzed by fluorescence microscopy to assess meiotic progression. Oocytes from the GV breakdown to the metaphase I stage were classified as intermediate; oocytes at the anaphase I, telophase I, and metaphase II stages as mature; and oocytes that could not be identified as being at any of the previous stages as degenerate (Luciano et al., 2011).

Assessment of labile zinc content in the oocytes

Labile zinc content in oocytes with different degree of chromatin compaction at the time of collection was assessed using the cell permeant zinc indicator FluoZin™3-AM dye (Molecular Probes, Termo Fisher Scientific), which had previously been used for spatial and temporal resolution of labile zinc concentrations in both mouse and bovine oocytes (Kim et al., 2011, Lisle et al., 2013, Que et al., 2019). Further validation of the FluoZin™3-AM using the zinc chelator TPEN is reported in supplemental Figure 1. After collection, COCs from early and medium antral follicles were incubated in 2 μM of FluoZin-3 and mixed to an equal volume of Pluronic® F-127 20% solution in DMSO (Invitrogen, Molecular Probes, Thermo Fisher Scientific) dissolved in 500 μL of M199 with 25 mM $NaHCO_3$ and supplemented with 0.68 mM L-glutamine, 0.4% fatty acid-free BSA, 0.2 mM sodium pyruvate, 0.1 mM cysteamine, 50 μg/mL kanamycin and 0.5 mM IBMX, in 4-well dishes at 38.5 °C under 5% CO_2 in humidified air for 90 min. After 1-hour incubation 1 μg/mL of Hoechst 33342 was added to each well. Subsequently, COCs were denuded mechanically by pipetting to remove cumulus cells in M199D supplemented with IBMX and 1 μg/mL of Hoechst 33342. Oocytes were placed on slides in 10 μL drops of the same medium and covered with a coverslip using secure-seal spacer (Invitrogen, Thermo Fisher Scientific). Digital images of each samples were immediately acquired using an epifluorescence microscope (Nikon Eclipse E600, Nikon, Tokyo, Japan) equipped with a digital camera (Nikon DS-F12) maintaining identical acquisition settings for all samples. All the images were acquired at the focal plane in which the chromatin was more focused. The oocyte labile zinc content was estimated by assessing the mean fluorescent intensity value emitted by the probe using ImageJ software (1.49v). The Total Fluorescent intensity emitted by the oocyte area (integrated density) was subtracted by the background and then normalized by the oocyte area. Mean Fluorescent intensity values were Log2 transformed. GV stages were classified according to the degree of chromatin compaction, as previously described (Lodde et al., 2007). The GV0 stage is characterized by a diffuse filamentous pattern

of chromatin in the whole nuclear area; the GV1 stage shows a few points of chromatin condensation; the GV2 stage has the chromatin condensed in distinct clumps; the GV3 stage is the highest levels of compaction with chromatin organized in a single clump within the nuclear envelope (Luciano and Lodde, 2013).

Assessment of global transcriptional activity

Transcription was assessed in growing oocytes cultured as COCs in IVCO medium as described above, in the presence or absence of zinc sulphate for 17h. In a second set of experiments, transcription was evaluated in oocytes treated with 10 μM zinc chelator TPEN, in the absence or presence of zinc sulphate for 5 h to prove TPEN specificity as previously described (Kim et al., 2010) . Global transcriptional activity was evaluated using the Click-iT® RNA Imaging Kit (Invitrogen, Thermo Fisher Scientific), as previously described in mice (Sanchez et al., 2015) and following the manufacture's guide.

Briefly, after treatment, COCs were incubated with 2 mM 5-ethynyl uridine (EU) diluted in IVCO medium for 1 h at 38.5°C 5%CO_2. Note that zinc and/or TPEN were included in the medium during EU incorporation, according to the experimental design. After EU incorporation, cumulus cells were mechanically removed, oocytes were briefly washed in warm PBS/PVA, fixed in 4% paraformaldehyde in PBS for 30 min at room temperature, and washed again in PBS/PVA. For detection of EU incorporation into nascent RNA, samples were permeabilized in 0.5% Triton-X 100 in PBS for 15 min at room temperature, briefly washed in PBS/PVA and incubated in Click-iT® reaction cocktail for 30 min at RT protected from light, further washed once in Click-iT® reaction rinse buffer and once more in PBS/PVA. Oocytes were finally mounted and stained in mounting media Vectashield antifade mounting media with DAPI (Vector, Burlingame, CA, USA), using double-sticky tape between the slide and the cover glass. Samples were analyzed and imaged under an epifluorescence microscope as

described above, maintaining identical acquisition settings for all the samples. Chromatin configuration was evaluated under the fluorescence microscope. The GV stage was classified according to the degree of chromatin compaction, as previously described (Lodde et al., 2007). The level of global transcriptional activity was estimated by assessing the mean fluorescent intensity value emitted by the incorporated EU using NIH ImageJ software (1.49v) (Schneider et al., 2012). The mean Fluorescent intensity emitted by the nuclear area was subtracted by the mean background intensity of the oocyte's cytoplasm. Note that transcription was quantified only in oocytes that retained a GV0 configuration during culture

Assessment of global DNA methylation

Levels of global DNA methylation were assessed by indirect immunofluorescence as previously described (Lodde et al., 2009) in oocytes subjected to IVCO for 17 h in the presence or absence of zinc sulphate. Briefly, after culture as COC, the oocytes were freed of cumulus cells and the zona pellucida was digested with 0.5% of pronase. Samples were then fixed in 4% paraformaldehyde in PBS for 1 h at 4°C, washed in 0.05% Tween 20 in PBS, permeabilized with 0.2% Triton X100, 0.05% Tween 20 in PBS for 30 min at room temperature, treated in 2 M HCl for 30 min at room temperature to obtain DNA denaturation and then neutralized in 100 mM Tris HCl buffer (pH 8.5) for 10 min. Non-specific binding was blocked by incubating the samples in 20% normal donkey serum, 1% BSA in PBS for 1 h at room temperature before primary antibody incubation. The samples were incubated overnight at 4°C with a mouse anti-5-methylcytosine (Eurogentec SA, Seraing Belgium) 1:500 in PBS containing 1% BSA and 0.05% Tween 20. Samples were extensively washed in 0.05% Tween 20 in PBS and incubated for 1 h at RT with a donkey anti mouse conjugated with Alexa Fluor 488 (Molecular Probes, Thermo Fisher Scientific, 1:500) in PBS containing 1% BSA and 0.05% Tween 20. Samples were mounted in Vecta Shield supplemented with DAPI, incubated for 5 minutes at room

temperature and immediately observed under epifluorescence microscopy. Images were captured under the same exposure conditions. The level of global DNA methylation was estimated by assessing the mean fluorescent intensity value emitted by the incorporated EU using NIH ImageJ software (1.49v) (Schneider et al., 2012). The mean Fluorescent intensity emitted by the nuclear area was subtracted by the mean background intensity of the oocyte's cytoplasm. Note that DNA methylation was quantified only in oocytes that retained a GV0 configuration.

Statistical analysis

Experiments were run in 3 independent experiments, unless otherwise specified. Statistical analysis was performed using GraphPad Prism software (GraphPad Prism v. 8, La Jolla, CA, USA). Data were pooled and expressed as mean ± SEM. Data were firstly analyzed by D'Agostino & Pearson test, in order assess whether data distribution was normal. Parametric tests (Student's t test and one-way ANOVA followed by Tukey's Multiple Comparison test) were used to determine differences when data where normally distributed. A non-parametric test (Mann Whitney test) was chosen when the data were not normally distributed or assumption on distribution could not be made. In the experiments where the labile zinc content was evaluated, values were Log2 transformed. Details on the statistical analysis are indicated in the figure caption. $P<0.05$ were considered statistically significant and indicated as *. Further differences, $P<0.01$, $P<0.001$, $P<0.0001$ are noted as **, *** and ****, respectively.

Results

Zinc transporters and metallothionein's encoding mRNAs are differentially expressed during oocyte growth and differentiation

To gain insights into the possible role of zinc during oocyte growth and differentiation that occur within the antral follicle before meiotic resumption, we mined the EmbryoGENE Profiler to assess the expression profiles of genes that encode for proteins that modulate zinc homeostasis in mammalian cells (Kimura and Kambe, 2016, Maret, 2017). Specifically, two major classes of ion transporters participate in this process: the SLC39A family members, which encode for ZIP proteins that transport zinc into the cytosol from either the extracellular space or intracellular stores such as the endoplasmic reticulum, and the SLC30A family members, which encode for the ZnT proteins that mediate zinc efflux from the cytosol (Kimura and Kambe, 2016). Moreover, MTs bind metals intracellularly, thus lowering their concentration at critical sites, or function as buffering molecules providing labile zinc for use by target proteins or enzymes when zinc is limited (Kimura and Kambe, 2016). Thus, the EmbryoGene profiler was mined to assess the expression profile of the known members of the *SLC39A*, *SLC30A* and *MT* gene families in oocytes collected from follicle of different size (Labrecque et al., 2016) as well as in oocytes with different degree of chromatin compaction and in their surrounding cumulus cells (Labrecque et al., 2015, Dieci et al., 2016).

As summarized in **Table 1**, the expression profiles of 21, 14 and 6 probes (representing constitutive, alternative 3'UTR and splicing variants) of the *SLC39A*, *SLC30A* and *MT* gene families were considered, respectively. Of these, several transcripts were differentially expressed in oocytes (Figure 1A and B). Specifically, *SLC39A7*/ZIP7, *SLC39A8*/ZIP8, *SLC39A10/*ZIP10 (both constitutive and alternative 3'UTR forms), *SLC39A12*/ZIP12, *SLC39A14/*ZIP14 (alternative 3'UTR), *SLC30A1/*ZnT1, *SLC30A5/*ZnT5 were differentially expressed according to follicle size and the degree of chromatin compaction. Furthermore *SLC39A6/*ZIP6, *SLC39A10/*ZIP10 (Alternative 3'UTR) and *SLC30A9/*ZnT9 were differentially expressed uniquely in oocytes derived from follicle of different size (**Figure 1A**), while

SLC39A9/ZIP9 (alternative 3'UTR), *SLC30A3*/ZnT3, *SLC30A6*/ZnT6 and *SLC30A7*/ZnT7 were differentially expressed uniquely in oocytes with different degree of chromatin compaction (**Figure 1B**). A lower number of genes, namely *SLC39A7*/ZIP7, *SLC39A8*/ZIP8, *SLC39A14*/ZnT14 alternative 3'UTR and *SLC30A4*/ZnT4, were differentially expressed in cumulus cells according to chromatin configuration (**Figure 1C**).

Zinc supplementation improves the meiotic competence of growing oocytes

Unlike fully-grown oocytes isolated from middle antral follicles, bovine oocytes collected from early antral follicles are not capable of spontaneously resuming meiosis once isolated from the follicular compartment and progressing to the MII stage. However, their ability to undergo meiosis and early embryonic development is, at least partially, enhanced when oocytes are cultured for 24 h before in vitro maturation in a low FSH concentration-based culture system that sustains oocyte-cumulus cells coupling (Luciano et al., 2011). To the best of our knowledge this is one of the few available culture systems for this class of oocytes. In the present study we used this culture system as experimental model to further assess the role of zinc during oogenesis. Preliminary experiments showed a detrimental/toxic effect of long-term treatment with the zinc chelator TPEN, as none of the oocytes exposed to IVCO supplemented with TPEN for 24 h was able to progress through meiosis when further subjected to standard IVM and, instead appeared degenerated. Therefore, we focused our attention on the effects of supplementing the IVCO medium with zinc and evaluating the effect on meiotic progression after standard IVM.

As shown in **Figure 2**, zinc supplementation induced a significantly higher percentage of mature oocytes and a lower percentage of oocytes at intermediated stages of meiotic progression, when compared to the control group. No differences were observed in the percentage of oocytes that did not resume meiosis nor in the degenerated class.

Labile zinc content decreases during physiological transcriptional silencing

The increased meiotic competence in response to zinc supplementation during IVCO suggests that zinc supports some of the processes that play a role in oocyte competence acquisition. Typically, the high majority (around 80%) of growing oocytes have their chromatin organized in a GV0 configuration and are transcriptionally active (Luciano et al., 2011, Lodde et al., 2008, Lodde et al., 2007, Fair et al., 1996, Fair et al., 1995). Therefore, we hypothesized that zinc supplementation might support transcription in GV0 oocytes. We tested this hypothesis using two experimental approaches.

First, we evaluated the labile zinc content in oocytes with different degrees of chromatin compaction at the time of isolation form early and middle antral follicles, since a major transcriptional silencing occurs during the transition from GV0 to GV1 stages and GV1, GV2 and GV3 oocytes are typically collected from middle antral follicles (Lodde et al., 2008, Lodde et al., 2007). As shown in **Figure 3**, quantification of the FluoZin™3-AM dye signal fluorescent intensity revealed a significant decrease of labile zinc content during the transition from GV0 to GV1 oocytes. Labile zinc remained low in GV2 oocytes, while tended to increase again in GV3 oocytes (**Figure 3B**).

Modulation of zinc availability affects global transcriptional activity

To more directly evaluate the role of zinc in the modulation of oocyte's transcription, in a second set of experiments, we supplemented the IVCO medium with zinc and/or with the zinc chelator TPEN and assessed global transcription in GV0 oocytes by means of EU incorporation into nascent RNA. As shown in **Figure 4A** this method clearly allowed the detection of RNA transcription in bovine oocytes. At the time of isolation, a positive signal was detectable only in GV0 oocytes and not in the negative control or fully-grown GV1 oocytes. Zinc

supplementation for 17 hours did not change the distribution of GV stages, and the percentage of GV0 oocytes remained high in both control and zinc supplemented group (**Figure 4C**). Importantly, quantification of the fluorescent signal revealed that global transcription was enhanced in the zinc treated group (**Figure 4D, E**).

When oocytes were exposed to the cell permeant zinc chelator TPEN, the level of global transcription significantly decreased (**Figure 5**, further supporting the hypothesis of a role of zinc in sustaining the transcriptional activity in growing oocytes. Notably, and as a control of the specificity of TPEN activity in acting as a zinc chelator, the TPEN effect was rescued by zinc supplementation, that restored the global transcription at levels comparable with the control group (**Figure 5C**).

Zinc supplementation affects global DNA methylation

Notably, we did not observe gross morphological changes of the chromatin configuration after zinc supplementation under epifluorescence microscopy. Therefore, to further assess the effects of zinc supplementation on chromatin structure, we assessed the level of global DNA methylation in oocytes subjected to IVCO in the presence or absence of zinc, as DNA methylation well correlates with transcriptional activity (reviewed in(Sendzikaite and Kelsey, 2019)). As shown in **Figure 6**, the level of global DNA methylation is significantly lower in GV0 oocytes cultured in the presence of zinc when compared to that observed in oocytes cultured in control IVCO condition. This results well correlates with higher levels of transcription in response to zinc supplementation.

Discussion

The major finding of the present study is that altering zinc availability, by means of culture medium supplementation during the final phase of their growth, supports global

transcriptional activity, modulates global DNA methylation and ultimately enhances acquisition of meiotic competence. Specifically, the present data indicate that the population of bovine oocytes that benefit from zinc supplementation during culture are the ones still engaged in accumulating substances for further development that are collected from early antral follicles. The final period of growth and differentiation is a crucial phase for the oocyte, as the epigenome is profoundly remodelled. Remodelling includes large-scale morphological re-organization of the chromatin to form the karyosphere (Bogolyubov, 2018), global transcriptional silencing as well as epigenetic modifications of DNA, such as DNA methylation, and histones proteins (De La Fuente, 2006, Luciano and Lodde, 2013, Tomizawa et al., 2012, O'Doherty et al., 2012). These modifications ultimately confer the oocyte with an appropriate developmental programme.

Preliminary indication of the importance of zinc homeostasis, which in mammalian cells is performed by carrying zinc across cell compartments, during oocyte growth, was revealed by the assessment of gene expression profiles of zinc transporters and methallotionein in the EmbryoGENE transcriptomic platform. To the best of our knowledge, excluding data on *SLC39A6/*ZIP6 and *SLC39A10/*ZIP10 (Kong et al., 2014) during murine oocyte maturation, no data are available on the function of other zinc transporters or MTs during mammalian oogenesis. An interesting hypothesis in the context of ovarian function is that different cellular compartments of the follicle cooperate to modulate zinc content in the follicular fluid, and ultimately in the germ cell. In this view, the EmbryoGENE profiler provides interesting targets to be further functionally characterized. For instance, *SLC39A8,* which encodes for ZIP8, would deserve further attention since it is differentially expressed also in granulosa cells at different stages of follicle development as reported by the EmbryoGENE Profiler, (http://emb-bioinfo.fsaa.ulaval.ca/IMAGE/cgi-bin/DoProfile.cgi?gene=slc39a8&tissue=granulosa, July 28, 2019).

Even though the characterization of zinc transporters and MTs mRNA expression profiles is not sufficient to predict the overall zinc balance in growing oocytes, the evidences that several zinc related transcripts are differentially expressed during this period, in both the oocyte and the surrounding cumulus cells, suggests that COCs actively control the abundance of these mRNAs, probably to modulate zinc signaling even long before meiotic resumption. This would lead to the statement that zinc availability in in vitro systems aimed to support oocyte growth has been underestimated so far. To the best of our knowledge, apart from the one developed in our laboratory and used as a base in the present study (Luciano et al., 2011), just few other studies focused on the in vitro culture of growing oocytes isolated from early antral follicles (Makita and Miyano, 2014, Hirao et al., 2004, Alam et al., 2018, Alm et al., 2006, Endo et al., 2013), while others had focused on culture of preantral oocytes. None of the published protocols can fully support embryonic developmental competence of growing oocytes. However, with the exception of serum-supplemented media, attempts to grow oocytes in vitro have been generally performed in the absence of zinc. In this study, we demonstrate that zinc supplementation to the IVCO system described by (Luciano et al., 2011) benefits the acquisition of meiotic competence. This result is highly relevant in the context of modern cattle farming, which is increasingly relying on in vitro embryo production (Blondin, 2015, Perry, 2017). In the practice, only fully-grown oocytes, which are directly subjected to IVM, are exploited. Conversely, growing oocytes contained in early antral follicles are generally discarded due to the lack of vitro culture systems able to support their development thus reducing the possibility of exploiting the ovarian reserve more efficiently (Lussier et al., 1987, Monget et al., 2012, Silva-Santos et al., 2011). Hence, our findings provide insights on how to improve culture media and strategies of assisted reproduction in livestock. Moreover, given the relevance of the bovine model to human ovarian physiology (Langbeen et al., 2015, Polejaeva et al., 2016), our findings would likely aid studies aimed at treating human infertility.

Defining the mechanism(s) by which zinc supports the acquisition of meiotic competence is not an easy task, due to the vast number of biological processes in which it is implicated (Beyersmann and Haase, 2001). Indeed, it has been estimated that around 2800 human proteins potentially bind zinc in vivo, which account for 10% of the human proteome (Andreini et al., 2006). Therefore, we focused our attention on one of the most important process occurring in the growing oocytes: transcription, which must be active to allow accumulation of large amounts of RNAs and proteins during growth and must be silenced timely in preparation for meiotic resumption. Zinc is a well-known regulator, acting both as activator and repressor, of gene expression machinery (Jackson et al., 2008, Andrews, 2001) and epigenetic modification, as many DNA modifiers enzymes bear zinc fingers motifs (Hudson and Buck-Koehntop, 2018, Rausch et al., 2019, Blanquart et al., 2019). Its role in controlling transcription has been considered also in the context of development of model organisms (Falchuk, 1998) as well as in the mouse preimplantation embryo, where it has been shown that TPEN-induced zinc insufficiency during in vitro culture was associated with altered chromatin structure in the blastomere nuclei and decreased global transcription (Kong et al., 2015). Moreover, in the mouse model, it has been shown that transcriptionally active oocytes react to changes of zinc availability by modulating the localization of the zinc sensor MTF-1(Kong et al., 2014) presumably to control zinc homeostasis (Andrews, 2001). The present study expands these observations by showing that major transcriptional silencing in bovine oocytes, which in vivo occurs during the transition from GV0 to GV1 configuration, is associated to a decrease of labile zinc content. Accordingly, a short-term treatment with zinc chelator TPEN induces a sudden reduction of transcription which is rescued by zinc supplementation. This might suggest that the signals that lead to transcriptional silencing in oocytes involves, at least in part, a decrease in labile zinc. Interestingly, labile zinc remains relatively low in GV2 oocytes, while it increases in GV3 oocytes, in which transcription is

completely silenced (Lodde et al., 2008). This agrees with the previously postulated hypothesis that increased chromatin condensation may reinforce transcriptional repression once it is initiated (De La Fuente, 2006, Luciano and Lodde, 2013). If so, we can speculate that GV3 oocytes would not be sensitive to increased labile zinc content, which in turn might correlate with increase of total zinc required during maturation in both cow and mice (Kim et al., 2010, Que et al., 2019). This hypothesis needs to be tested. Moreover, it will be of utmost importance to assess whether oocytes with different chromatin configurations vary in terms of total zinc content, as described in (Que et al., 2019)

Importantly we provide evidences that zinc supplementation enhances transcription in cultured GV0 oocytes, which well correlates with the maintenance of global level of DNA methylation that is known to characterize GV0 oocytes at the time of collection (Lodde et al., 2009). This likely accounts, at least in part, for the increased meiotic competence of zinc treated oocytes in our experimental model. Future mechanistic studies should be conducted to further clarify whether zinc supplementation affects the amount of labile and total zinc in the oocyte and, importantly, in the surrounding cumulus cells and thus clarify the molecular mechanisms through which zinc enhance oocyte capacity to undergo maturation. Nevertheless, our finding could be exploited to further ameliorate the cultural system, aiming at prolonging the period in which the oocytes remain transcriptionally active while allowing timely transcriptional silencing when the oocytes have accumulated the critical molecules for subsequent development.

Conclusion

A relationship between zinc deficiency and infertility in dairy cows has been known from many years; zinc deficiency results in increased embryonic mortality and reduced conception rates (Hidiroglou, 1979). This might be due, at least in part, to the role that zinc

plays in oocyte development, although the mechanisms are not completely elucidated. Here we provide evidences that zinc modulates transcription during a critical step of oocyte development, which is when its developmental program is largely determined. Our results agree with previous findings in mice, where feeding a zinc deficient diet during preconception (3–5 days before ovulation) alters oocyte chromatin methylation (histone H3K4 trimethylation and global DNA methylation) and expression of specific genes (Tian and Diaz, 2013).

Clearly, it is likely that zinc participate in many other biological functions in the growing oocytes such as mitochondrial function and metabolism regulation, and might have Antioxidant/Prooxidant activity (Lee, 2018). Further studied are required to assess this hypothesis. Finally, of outmost importance will be the assessment of which are the relative contributions of the cumulus cells and the oocytes to the maintenance of zinc homeostasis during oogenesis as well as the characterization of specific biomarkers that primarily control importance of zinc transport and storage during oogenesis.

Declaration of interest

Authors declare that there is no conflict of interest that could be perceived as prejudicing the impartiality of the research reported.

Funding

V.L. acknowledges the receipt of a fellowship from the OECD Co-operative Research Programme: Biological Resource Management for Sustainable Agricultural Systems in 2016 (contract n. JA00091594), which supported part of this study. Part of the experiments were funded by the “Piano Strategico Linea B” of the University of Milan (PSR2019_DIP_AMLUC to A.M.L, PSR2018_DIP_027_VLODD to V.L., and PSR2018_DIP_027_FFRAN to F.F.). P.C.D.A was supported by Scholarship from Capes

foundation /PDSE/88881.134900/2016-01. EmbryoGENE Strategic Network was funded by Natural Sciences and Engineering Research Council of Canada (NSERC), Canada. C.R. acknowledges the Natural Sciences and Engineering Research Council of Canada (RGPIN-2017-04775)

Author's contribution

VL and AML conceived the study. CD and VL participated in EmbryoGENE data analysis. MAS contributed to the study design and EmbryoGene data Analysis. RGB, VL and AML performed experiments on the assessment of the effect of zinc supplementation on meiotic competence and DNA methylation. PCDA, AB CR and VL performed experiments on the assessment on labile zinc content in oocytes. PCDA and FF performed experiments on the assessment of transcriptional activity. VL wrote the manuscript. All authors reviewed and approved the manuscript

Acknowledgements

Authors are grateful to INALCA S.p.A. (Ospedaletto Lodigiano, LO) and support of the Veterinary staff. We would like to thank all the scientists of the EmbryoGENE Network that contributed in creating the EmbryoGENE profiler.

References

ALAM, M. H., LEE, J. & MIYANO, T. 2018. Inhibition of PDE3A sustains meiotic arrest and gap junction of bovine growing oocytes in in vitro growth culture. *Theriogenology,* 118**,** 110-118.

ALM, H., KATSKA-KSIAZKIEWICZ, L., RYNSKA, B. & TUCHSCHERER, A. 2006. Survival and meiotic competence of bovine oocytes originating from early antral ovarian follicles. *Theriogenology,* 65**,** 1422-34.

ANCHORDOQUY, J. M., ANCHORDOQUY, J. P., SIRINI, M. A., PICCO, S. J., PERAL-GARCIA, P. & FURNUS, C. C. 2014. The importance of having zinc during in vitro maturation of cattle cumulus-oocyte complex: role of cumulus cells. *Reprod Domest Anim,* 49**,** 865-74.

ANDREINI, C., BANCI, L., BERTINI, I. & ROSATO, A. 2006. Counting the zinc-proteins encoded in the human genome. *J Proteome Res,* 5**,** 196-201.

ANDREWS, G. K. 2001. Cellular zinc sensors: MTF-1 regulation of gene expression. *Biometals,* 14**,** 223-37.

BERNHARDT, M. L., KIM, A. M., O'HALLORAN, T. V. & WOODRUFF, T. K. 2011. Zinc requirement during meiosis I-meiosis II transition in mouse oocytes is independent of the MOS-MAPK pathway. *Biol Reprod,* 84**,** 526-36.

BERNHARDT, M. L., KONG, B. Y., KIM, A. M., O'HALLORAN, T. V. & WOODRUFF, T. K. 2012. A zinc-dependent mechanism regulates meiotic progression in mammalian oocytes. *Biol Reprod,* 86**,** 114.

BEYERSMANN, D. & HAASE, H. 2001. Functions of zinc in signaling, proliferation and differentiation of mammalian cells. *Biometals,* 14**,** 331-41.

BLANQUART, C., LINOT, C., CARTRON, P. F., TOMASELLI, D., MAI, A. & BERTRAND, P. 2019. Epigenetic Metalloenzymes. *Curr Med Chem,* 26**,** 2748-2785.

BLONDIN, P. 2015. Status of embryo production in the world. *Anim Reprod,* 12**,** 356-358.

BOGOLYUBOV, D. S. 2018. Karyosphere (Karyosome): A Peculiar Structure of the Oocyte Nucleus. *Int Rev Cell Mol Biol,* 337**,** 1-48.

DE LA FUENTE, R. 2006. Chromatin modifications in the germinal vesicle (GV) of mammalian oocytes. *Dev Biol,* 292**,** 1-12.

DEAN, K. M., QIN, Y. & PALMER, A. E. 2012. Visualizing metal ions in cells: an overview of analytical techniques, approaches, and probes. *Biochim Biophys Acta,* 1823**,** 1406-15.

DIECI, C., LODDE, V., LABREQUE, R., DUFORT, I., TESSARO, I., SIRARD, M. A. & LUCIANO, A. M. 2016. Differences in cumulus cell gene expression indicate the benefit of a pre-maturation step to improve in-vitro bovine embryo production. *Mol Hum Reprod,* 22**,** 882-897.

DUNCAN, F. E., QUE, E. L., ZHANG, N., FEINBERG, E. C., O'HALLORAN, T. V. & WOODRUFF, T. K. 2016. The zinc spark is an inorganic signature of human egg activation. *Sci Rep,* 6**,** 24737.

ENDO, M., KAWAHARA-MIKI, R., CAO, F., KIMURA, K., KUWAYAMA, T., MONJI, Y. & IWATA, H. 2013. Estradiol supports in vitro development of bovine early antral follicles. *Reproduction,* 145**,** 85-96.

FAIR, T., HYTTEL, P. & GREVE, T. 1995. Bovine oocyte diameter in relation to maturational competence and transcriptional activity. *Mol Reprod Dev,* 42**,** 437-42.

FAIR, T., HYTTEL, P., GREVE, T. & BOLAND, M. 1996. Nucleus structure and transcriptional activity in relation to oocyte diameter in cattle. *Mol Reprod Dev,* 43**,** 503-12.

FALCHUK, K. H. 1998. The molecular basis for the role of zinc in developmental biology. *Mol Cell Biochem,* 188**,** 41-8.

HIDIROGLOU, M. 1979. Trace element deficiencies and fertility in ruminants: a review. *J Dairy Sci,* 62**,** 1195-206.
HIRAO, Y., ITOH, T., SHIMIZU, M., IGA, K., AOYAGI, K., KOBAYASHI, M., KACCHI, M., HOSHI, H. & TAKENOUCHI, N. 2004. In vitro growth and development of bovine oocyte-granulosa cell complexes on the flat substratum: effects of high polyvinylpyrrolidone concentration in culture medium. *Biol Reprod,* 70**,** 83-91.
HUDSON, N. O. & BUCK-KOEHNTOP, B. A. 2018. Zinc Finger Readers of Methylated DNA. *Molecules,* 23.
JACKSON, K. A., VALENTINE, R. A., CONEYWORTH, L. J., MATHERS, J. C. & FORD, D. 2008. Mechanisms of mammalian zinc-regulated gene expression. *Biochem Soc Trans,* 36**,** 1262-6.
JEON, Y., YOON, J. D., CAI, L., HWANG, S. U., KIM, E., ZHENG, Z., JEUNG, E., LEE, E. & HYUN, S. H. 2015. Zinc deficiency during in vitro maturation of porcine oocytes causes meiotic block and developmental failure. *Mol Med Rep,* 12**,** 5973-82.
KHAN, D. R., FOURNIER, E., DUFORT, I., RICHARD, F. J., SINGH, J. & SIRARD, M. A. 2016. Meta-analysis of gene expression profiles in granulosa cells during folliculogenesis. *Reproduction,* 151**,** R103-10.
KIM, A. M., BERNHARDT, M. L., KONG, B. Y., AHN, R. W., VOGT, S., WOODRUFF, T. K. & O'HALLORAN, T. V. 2011. Zinc sparks are triggered by fertilization and facilitate cell cycle resumption in mammalian eggs. *ACS Chem Biol,* 6**,** 716-23.
KIM, A. M., VOGT, S., O'HALLORAN, T. V. & WOODRUFF, T. K. 2010. Zinc availability regulates exit from meiosis in maturing mammalian oocytes. *Nat Chem Biol,* 6**,** 674-81.
KIMURA, T. & KAMBE, T. 2016. The Functions of Metallothionein and ZIP and ZnT Transporters: An Overview and Perspective. *Int J Mol Sci,* 17**,** 336.
KONG, B. Y., BERNHARDT, M. L., KIM, A. M., O'HALLORAN, T. V. & WOODRUFF, T. K. 2012. Zinc maintains prophase I arrest in mouse oocytes through regulation of the MOS-MAPK pathway. *Biol Reprod,* 87**,** 11, 1-12.
KONG, B. Y., DUNCAN, F. E., QUE, E. L., KIM, A. M., O'HALLORAN, T. V. & WOODRUFF, T. K. 2014. Maternally-derived zinc transporters ZIP6 and ZIP10 drive the mammalian oocyte-to-egg transition. *Mol Hum Reprod,* 20**,** 1077-89.
KONG, B. Y., DUNCAN, F. E., QUE, E. L., XU, Y., VOGT, S., O'HALLORAN, T. V. & WOODRUFF, T. K. 2015. The inorganic anatomy of the mammalian preimplantation embryo and the requirement of zinc during the first mitotic divisions. *Dev Dyn,* 244**,** 935-47.
LABRECQUE, R., FOURNIER, E. & SIRARD, M. A. 2016. Transcriptome analysis of bovine oocytes from distinct follicle sizes: Insights from correlation network analysis. *Mol Reprod Dev,* 83**,** 558-69.
LABRECQUE, R., LODDE, V., DIECI, C., TESSARO, I., LUCIANO, A. M. & SIRARD, M. A. 2015. Chromatin remodelling and histone m RNA accumulation in bovine germinal vesicle oocytes. *Mol Reprod Dev,* 82**,** 450-62.
LANGBEEN, A., DE PORTE, H. F., BARTHOLOMEUS, E., LEROY, J. L. & BOLS, P. E. 2015. Bovine in vitro reproduction models can contribute to the development of (female) fertility preservation strategies. *Theriogenology,* 84**,** 477-89.
LEE, S. R. 2018. Critical Role of Zinc as Either an Antioxidant or a Prooxidant in Cellular Systems. *Oxid Med Cell Longev,* 2018**,** 9156285.
LISLE, R. S., ANTHONY, K., RANDALL, M. A. & DIAZ, F. J. 2013. Oocyte-cumulus cell interactions regulate free intracellular zinc in mouse oocytes. *Reproduction,* 145**,** 381-90.
LODDE, V., MODINA, S., GALBUSERA, C., FRANCIOSI, F. & LUCIANO, A. M. 2007. Large-scale chromatin remodeling in germinal vesicle bovine oocytes: interplay with gap junction functionality and developmental competence. *Mol Reprod Dev,* 74**,** 740-9.
LODDE, V., MODINA, S., MADDOX-HYTTEL, P., FRANCIOSI, F., LAURIA, A. & LUCIANO, A. M. 2008. Oocyte morphology and transcriptional silencing in relation to chromatin

remodeling during the final phases of bovine oocyte growth. *Mol Reprod Dev,* 75**,** 915-24.
LODDE, V., MODINA, S. C., FRANCIOSI, F., ZUCCARI, E., TESSARO, I. & LUCIANO, A. M. 2009. Localization of DNA methyltransferase-1 during oocyte differentiation, in vitro maturation and early embryonic development in cow. *Eur J Histochem,* 53**,** e24.
LUCIANO, A. M., FRANCIOSI, F., DIECI, C. & LODDE, V. 2014a. Changes in large-scale chromatin structure and function during oogenesis: a journey in company with follicular cells. *Anim Reprod Sci,* 149**,** 3-10.
LUCIANO, A. M., FRANCIOSI, F., DIECI, C., TESSARO, I., TERZAGHI, L., MODINA, S. C. & LODDE, V. 2014b. Large-scale chromatin structure and function changes during oogenesis: the interplay between oocyte and companion cumulus cells. *Anim Reprod,* 11**,** 141-149.
LUCIANO, A. M., FRANCIOSI, F., MODINA, S. C. & LODDE, V. 2011. Gap junction-mediated communications regulate chromatin remodeling during bovine oocyte growth and differentiation through cAMP-dependent mechanism(s). *Biol Reprod,* 85**,** 1252-9.
LUCIANO, A. M. & LODDE, V. 2013. Changes of Large-Scale Chromatin Configuration During Mammalian Oocyte Differentiation. *In:* COTICCHIO, G., ALBERTINI, D. F. & DE SANTIS, L. (eds.) *Oogenesis.* Springer London.
LUSSIER, J. G., MATTON, P. & DUFOUR, J. J. 1987. Growth rates of follicles in the ovary of the cow. *J Reprod Fertil,* 81**,** 301-7.
MAKITA, M. & MIYANO, T. 2014. Steroid hormones promote bovine oocyte growth and connection with granulosa cells. *Theriogenology,* 82**,** 605-12.
MARET, W. 2017. Zinc in Cellular Regulation: The Nature and Significance of "Zinc Signals". *Int J Mol Sci,* 18.
MONGET, P., BOBE, J., GOUGEON, A., FABRE, S., MONNIAUX, D. & DALBIES-TRAN, R. 2012. The ovarian reserve in mammals: a functional and evolutionary perspective. *Mol Cell Endocrinol,* 356**,** 2-12.
O'DOHERTY, A. M., O'SHEA, L. C. & FAIR, T. 2012. Bovine DNA methylation imprints are established in an oocyte size-specific manner, which are coordinated with the expression of the DNMT3 family proteins. *Biol Reprod,* 86**,** 67.
OUTTEN, C. E. & O'HALLORAN, T. V. 2001. Femtomolar sensitivity of metalloregulatory proteins controlling zinc homeostasis. *Science,* 292**,** 2488-92.
PERRY, A. C. 2017. 2016 STATISTICS OF EMBRYO COLLECTION AND TRANSFER IN DOMESTIC FARM ANIMALS. https://www.iets.org/comm_data.asp?autotry=true&ULnotkn=true.
PICCO, S. J., ANCHORDOQUY, J. M., DE MATOS, D. G., ANCHORDOQUY, J. P., SEOANE, A., MATTIOLI, G. A., ERRECALDE, A. L. & FURNUS, C. C. 2010. Effect of increasing zinc sulphate concentration during in vitro maturation of bovine oocytes. *Theriogenology,* 74**,** 1141-8.
POLEJAEVA, I. A., RUTIGLIANO, H. M. & WELLS, K. D. 2016. Livestock in biomedical research: history, current status and future prospective. *Reprod Fertil Dev,* 28**,** 112-24.
QUE, E. L., BLEHER, R., DUNCAN, F. E., KONG, B. Y., GLEBER, S. C., VOGT, S., CHEN, S., GARWIN, S. A., BAYER, A. R., DRAVID, V. P., WOODRUFF, T. K. & O'HALLORAN, T. V. 2015. Quantitative mapping of zinc fluxes in the mammalian egg reveals the origin of fertilization-induced zinc sparks. *Nat Chem,* 7**,** 130-9.
QUE, E. L., DUNCAN, F. E., BAYER, A. R., PHILIPS, S. J., ROTH, E. W., BLEHER, R., GLEBER, S. C., VOGT, S., WOODRUFF, T. K. & O'HALLORAN, T. V. 2017. Zinc sparks induce physiochemical changes in the egg zona pellucida that prevent polyspermy. *Integr Biol (Camb),* 9**,** 135-144.
QUE, E. L., DUNCAN, F. E., LEE, H. C., HORNICK, J. E., VOGT, S., FISSORE, R. A., O'HALLORAN, T. V. & WOODRUFF, T. K. 2019. Bovine eggs release zinc in response to parthenogenetic and sperm-induced egg activation. *Theriogenology,* 127**,** 41-48.

RAUSCH, C., HASTERT, F. D. & CARDOSO, M. C. 2019. DNA Modification Readers and Writers and Their Interplay. *J Mol Biol*.
SANCHEZ, F., ROMERO, S., DE VOS, M., VERHEYEN, G. & SMITZ, J. 2015. Human cumulus-enclosed germinal vesicle oocytes from early antral follicles reveal heterogeneous cellular and molecular features associated with in vitro maturation capacity. *Hum Reprod,* 30**,** 1396-409.
SCHNEIDER, C. A., RASBAND, W. S. & ELICEIRI, K. W. 2012. NIH Image to ImageJ: 25 years of image analysis. *Nat Methods,* 9**,** 671-5.
SENDZIKAITE, G. & KELSEY, G. 2019. The role and mechanisms of DNA methylation in the oocyte. *Essays Biochem,* 63**,** 691-705.
SILVA-SANTOS, K. C., SANTOS, G. M., SILOTO, L. S., HERTEL, M. F., ANDRADE, E. R., RUBIN, M. I., STURION, L., MELO-STERZA, F. A. & SENEDA, M. M. 2011. Estimate of the population of preantral follicles in the ovaries of Bos taurus indicus and Bos taurus taurus cattle. *Theriogenology,* 76**,** 1051-7.
TIAN, X., ANTHONY, K., NEUBERGER, T. & DIAZ, F. J. 2014. Preconception zinc deficiency disrupts postimplantation fetal and placental development in mice. *Biol Reprod,* 90**,** 83.
TIAN, X. & DIAZ, F. J. 2012. Zinc depletion causes multiple defects in ovarian function during the periovulatory period in mice. *Endocrinology,* 153**,** 873-86.
TIAN, X. & DIAZ, F. J. 2013. Acute dietary zinc deficiency before conception compromises oocyte epigenetic programming and disrupts embryonic development. *Dev Biol,* 376**,** 51-61.
TOMIZAWA, S., NOWACKA-WOSZUK, J. & KELSEY, G. 2012. DNA methylation establishment during oocyte growth: mechanisms and significance. *Int J Dev Biol,* 56**,** 867-75.
ZHAO, M. H., KWON, J. W., LIANG, S., KIM, S. H., LI, Y. H., OH, J. S., KIM, N. H. & CUI, X. S. 2014. Zinc Regulates Meiotic Resumption in Porcine Oocytes via a Protein Kinase C-Related Pathway. *PLoS One,* 9**,** e102097.
ZUCCOTTI, M., GARAGNA, S., MERICO, V., MONTI, M. & ALBERTO REDI, C. 2005. Chromatin organisation and nuclear architecture in growing mouse oocytes. *Mol Cell Endocrinol,* 234**,** 11-7.

Figure legends

Fig. 1 Levels of differentially expressed mRNAs encoding zinc transporters (ZIP and ZnT) and metallothioneins (MT) during oocyte growth and differentiation

Graphs showing changes of mRNA levels encoding the differentially expressed members of the SLC39A, SLC30A and MT gene families in oocytes collected from follicles of different sizes (**A**) and in oocytes and corresponding cumulus cells with different degrees of chromatin compaction (**B and C**). The data represent the profiles in the original microarray analysis and are obtained/imported from the EmbryoGENE profiler website (http://emb-bioinfo.fsaa.ulaval.ca/IMAGE/) on June 4th 2019. Data were generated by (Labrecque et al., 2016) and (Dieci et al., 2016, Labrecque et al., 2015).

Figure 2: Effect of zinc supplementation during IVCO on meiotic competence acquisition

(**A**) Schematic representation of the experimental design (**B**) Representative epifluorescent images showing immature (GV), intermediate (MI), Mature (MII, polar view and first polar body) and Degenerated oocytes as assessed by DNA staining with DAPI (**C**) Graphs showing the percentage of immature, intermediate, mature and degenerated oocytes in the Control (IVCO in the absence of zinc followed by standard IVM) and zinc (IVCO in the presence of zinc followed by standard IVM) groups. Data were analyzed by Mann-Whithney Test. Values are means ± SEM (n=6). * and ** indicates significant differences between groups (*P<0.05; ** P<0.01). A total of 98 and 102 oocytes were analyzed for Control and zinc groups, respectively in three independent experiments with two technical replicates each.

Figure 3: Relationship between large-scale chromatin configuration of the oocyte and labile zinc content

(A) Representative images showing chromatin staining by Hoechst33342 (upper and middle panels) and Labile zinc staining by Fluo Zin (Lower panel) in oocytes with GV0, GV1, GV2 and GV3 chromatin configuration. All Images were captured at the GV focal plane **(B)** Graph showing quantification of labile zinc content as assessed by Fluo Zin loading ad fluorescent image analysis in growing oocytes collected from small antral follicle with a GV0 chromatin configuration, and fully-grown oocytes collected from middle antral follicle with GV1, GV2 and GV3 chromatin configuration as assessed by Hoechst 33342 staining. Total numbers of oocytes analyzed are shown in brackets. Data were pooled together and analyzed by 1-way ANOVA followed by Tukey's multiple comparison test. Values are means ± SEM. * and ** indicate significant differences between groups (*P<0.05; **P<0.01).

Figure 4: Effect of zinc supplementation during IVCO on global transcriptional activity in GV0 oocytes

(**A**) Representative images showing chromatin staining by DAPI (upper panel) and EU incorporation (lower panel) in GV0 oocytes collected from small antral follicles in the absence (Negative CTRL, left panel) and presence of EU (positive CTRL, middle panel), as well as in a fully-grown oocyte collected from middle antral follicle with a GV1 chromatin configuration (right panel). Note that a positive signal is detected only in GV0 oocytes in the presence of EU. (**B**) Schematic representation of the experimental design (**C**) Graph showing the effect of zinc supplementation during 17h of culture on chromatin configuration and meiotic progression. Total numbers of oocytes analyzed in two independent experiments are indicated in the graph. Note that no differences were observed (**D**) Representative images showing chromatin staining by DAPI (upper panel) and transcription (lower panel) in GV0

oocytes after culture for 17 h under control IVCO condition or in the presence of zinc (**E**) Graph showing quantification of transcriptional activity as assessed by EU incorporation into nascent RNA and fluorescent image analysis in GV0 oocytes cultured in IVCO medium in the absence or presence of zinc. Data were analyzed by unpaired t-test; total number of oocytes analyzed are indicated in parentheses. Values are means ± SEM. ** indicate significant differences between groups (**P<0.01).

Figure 5: Effect of zinc chelation during 5h IVCO on global transcriptional activity in GV0 oocytes

(**A**) Schematic representation of the experimental design (**B**) Representative images of showing chromatin staining by DAPI (upper panel) and transcription (lower panel) in GV0 oocytes after culture for 5 h under control IVCO condition, in the presence of the zinc chelator TPEN or in the presence of TPEN + zinc (**B**) Graph showing quantification of transcriptional activity in GV0 oocytes cultured in IVCO medium for 5h (CTRL) and in IVCO medium supplemented by TPEN or TPEN + zinc. Data were analyzed by 1 way-ANOVA followed by Tukey's multiple comparison test; total number of oocytes analyzed in three independent experiments are indicated in parentheses. Values are means ± SEM. * and ** indicate significant differences between groups (*P<0.05; **P<0.01).

Figure 6: Effect of zinc supplementation during IVCO on global DNA methylation in GV0 oocytes

(**A**) Schematic representation of the experimental groups. (**B**) Representative images showing chromatin staining by DAPI (upper panel) and global DNA methylation (lower panel) in GV0 oocytes after culture in IVCO medium in the Control (IVCO medium) and Zinc (IVCO medium in the presence of zinc groups. (**C**) Graph showing quantification of global DNA

methylation as assessed by indirect immunofluorescence and image analysis in GV0 oocytes cultured in IVCO medium in the absence or presence of zinc. Data were analyzed by Mann-Whitney; total number of oocytes analyzed in two independent experiments are indicated in parentheses. Values are means ± SEM. **** indicate significant differences between groups ($P<0.0001$).

Figures/ tables.

Table 1:

List of zinc related targets identified within the EmbyoGENE profiler web site. The genes whose expression level is significantly affected by the follicular size in the oocyte (Labrecque et al., 2016), and by the chromatin status in the oocyte and the corresponding cumulus cells (Dieci et al., 2016, Labrecque et al., 2015), are marked in dark grey. Expression profiles for each of the indicated probe are shown in Figure 1 and can be assessed in the original dataset (http://emb-bioinfo.fsaa.ulaval.ca/IMAGE/). The dataset was last mined on June 4th 2019.

Gene of interest					**Cell type and variable considered in the microarray study**		
					Oocyte from follicle of different size	**Oocyte with different chromatin configuration**	**Cumulus cells isolated from oocytes with different chromatin configuration**
EmbryoGene Probe	**Gene symbol**	**Gene Name**	**Encoded protein Symbol**	**Type**	*Labrecque et al, MRD 2016*	*Labrecque et al, MRD 2015*	*Dieci et al, MHR 2016*
EMBV3_32972	***SLC39A1***	solute carrier family 39 member 1	**ZIP 1**	Constitutive			
EMBV3_18524	***SLC39A2***	solute carrier family 39 member 2	**ZIP 2**	Constitutive			
EMBV3_02694	***SLC39A3***	solute carrier family 39 member 3	**ZIP 3**	Constitutive			
EMBV3_12697	***SLC39A4***	solute carrier family 39 member 4	**ZIP 4**	Constitutive			
EMBV3_01886	***SLC39A5***	solute carrier family 39 member 5	**ZIP 5**	Constitutive			
EMBV3_09740	***SLC39A5***	solute carrier family 39 member 5	**ZIP 5**	Splicing variant			

EMBV3_02273	***SLC39A6***	solute carrier family 39 member 6	**ZIP 6**	Constitutive	*		
EMBV3_34613	***SLC39A7***	solute carrier family 39 member 7	**ZIP 7**	Constitutive	*	*	*
EMBV3_42354	***SLC39A8***	solute carrier family 39 member 8	**ZIP 8**	Constitutive	*	*	*
EMBV3_16082	***SLC39A9***	solute carrier family 39 member 9	**ZIP 9**	Alternative 3'UTR			
EMBV3_17943	***SLC39A9***	solute carrier family 39 member 9	**ZIP 9**	Constitutive			
EMBV3_24626	***SLC39A9***	solute carrier family 39 member 9	**ZIP 9**	Alternative 3'UTR		*	
EMBV3_15122	***SLC39A10***	solute carrier family 39 member 10	**ZIP 10**	Alternative 3'UTR	*		
EMBV3_29633	***SLC39A10***	solute carrier family 39 member 10	**ZIP 10**	Constitutive	*	*	
EMBV3_31415	***SLC39A10***	solute carrier family 39 member 10	**ZIP 10**	Alternative 3'UTR	*	*	
EMBV3_10318	***SLC39A11***	solute carrier family 39 member 11	**ZIP 11**	Constitutive			
EMBV3_21073	***SLC39A12***	solute carrier family 39 member 12	**ZIP 12**	Constitutive	*	*	
EMBV3_19564	***SLC39A13***	solute carrier family 39 member 13	**ZIP13**	Constitutive			
EMBV3_01984	***SLC39A14***	solute carrier family 39 member 14	**ZIP 14**	Constitutive			
EMBV3_03243	***SLC39A14***	solute carrier family 39 member 14	**ZIP 14**	Alternative 3'UTR	*	*	
EMBV3_12779	***SLC39A14***	solute carrier family 39 member 14	**ZIP 14**	Alternative 3'UTR			*
EMBV3_38125	***SLC30A1***	solute carrier family 30 member 1	**ZnT 1**	Alternative 3'UTR			
EMBV3_41937	***SLC30A1***	solute carrier family 30 member 1	**ZnT 1**	Alternative 3'UTR			
EMBV3_21137	***SLC30A1***	solute carrier family 30 member 1	**ZnT 1**	Constitutive	*	*	
EMBV3_40498	***SLC30A2***	solute carrier family 30 member 2	**ZnT 2**	Constitutive			
EMBV3_41101	***SLC30A2***	solute carrier family 30 member 2	**ZnT 2**	Splicing variant			
EMBV3_42173	***SLC30A3***	solute carrier family 30 member 3	**ZnT 3**	Constitutive		*	
EMBV3_18378	***SLC30A4***	solute carrier family 30 member 4	**ZnT 4**	Constitutive			*
EMBV3_16827	***SLC30A5***	solute carrier family 30 member 5	**ZnT 5**	Constitutive	*	*	
EMBV3_09102	***SLC30A6***	solute carrier family 30 member 6	**ZnT 6**	Constitutive		*	
EMBV3_12614	***SLC30A6***	solute carrier family 30 member 6	**ZnT 6**	Splicing variant			
EMBV3_36463	***SLC30A6***	solute carrier family 30 member 6	**ZnT 6**	Splicing variant			
EMBV3_18316	***SLC30A7***	solute carrier family 30 member 7	**ZnT 7**	Constitutive		*	

EMBV3_39734	***SLC30A9***	solute carrier family 30 member 9	**ZnT 9**	Constitutive	*		
EMBV3_02033	***SLC30A10***	solute carrier family 30 member 10	**ZnT 10**	Constitutive			
EMBV3_08028	***MT1A***	metallothionein-1A	**MT1A**	Constitutive			
EMBV3_07532	***MT1E***	metallothionein-1E	**MT1E**	Constitutive			
EMBV3_34220	***MT1E***	metallothionein-1E	**MT1E**	Constitutive			
EMBV3_06636	***MT2A***	metallothionein-2E	**MT2E**	Constitutive			
EMBV3_40027	***MT3***	metallothionein-3	**MT3**	Constitutive	*	*	
EMBV3_30913	***MT4***	metallothionein-4	**MT4**	Constitutive			

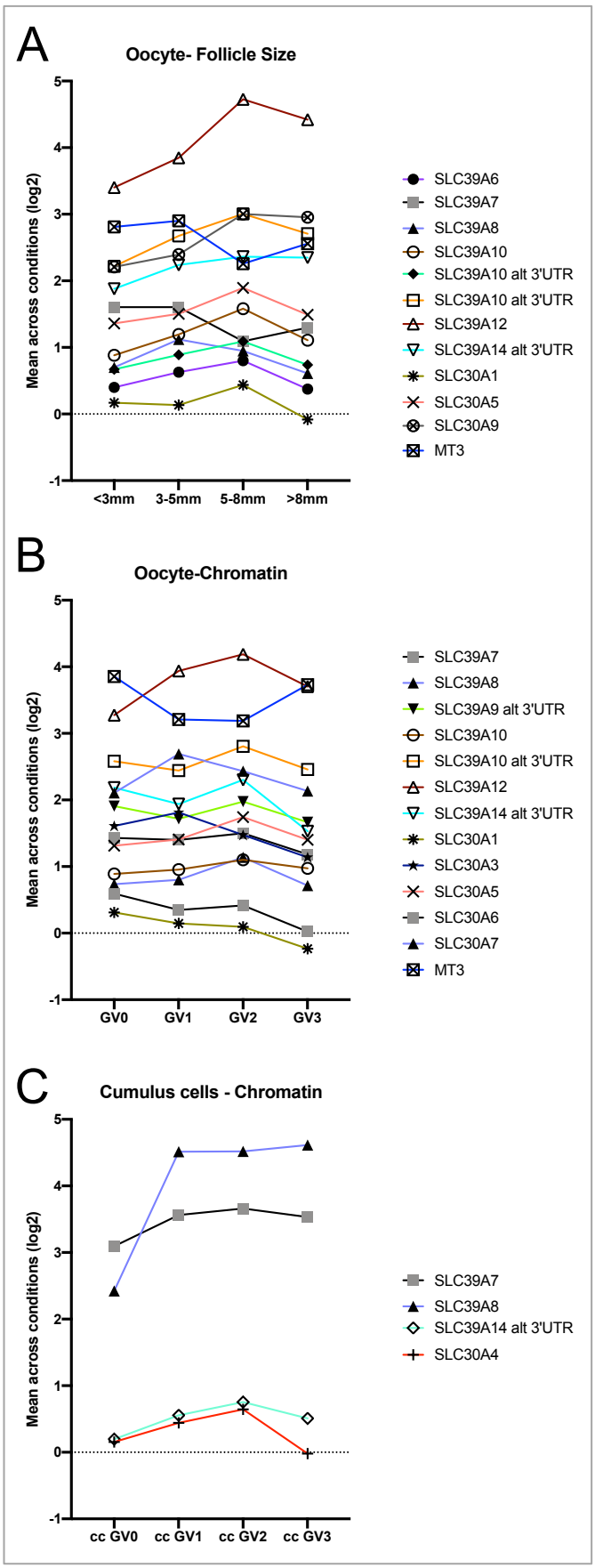

Fig. 1 Levels of differentially expressed mRNAs encoding zinc transporters (ZIP and ZnT) and metallothioneins (MT) during oocyte growth and differentiation

Graphs showing changes of mRNA levels encoding the differentially expressed members of the SLC39A, SLC30A and MT gene families in oocytes collected from follicles of different sizes (**A**) and in oocytes and corresponding cumulus cells with different degrees of chromatin compaction (**B and C**). The data represent the profiles in the original microarray analysis and are obtained/imported from the EmbryoGENE profiler website (http://emb-bioinfo.fsaa.ulaval.ca/IMAGE/) on June 4th 2019. Data were generated by (Labrecque et al., 2016) and (Dieci et al., 2016, Labrecque et al., 2015).

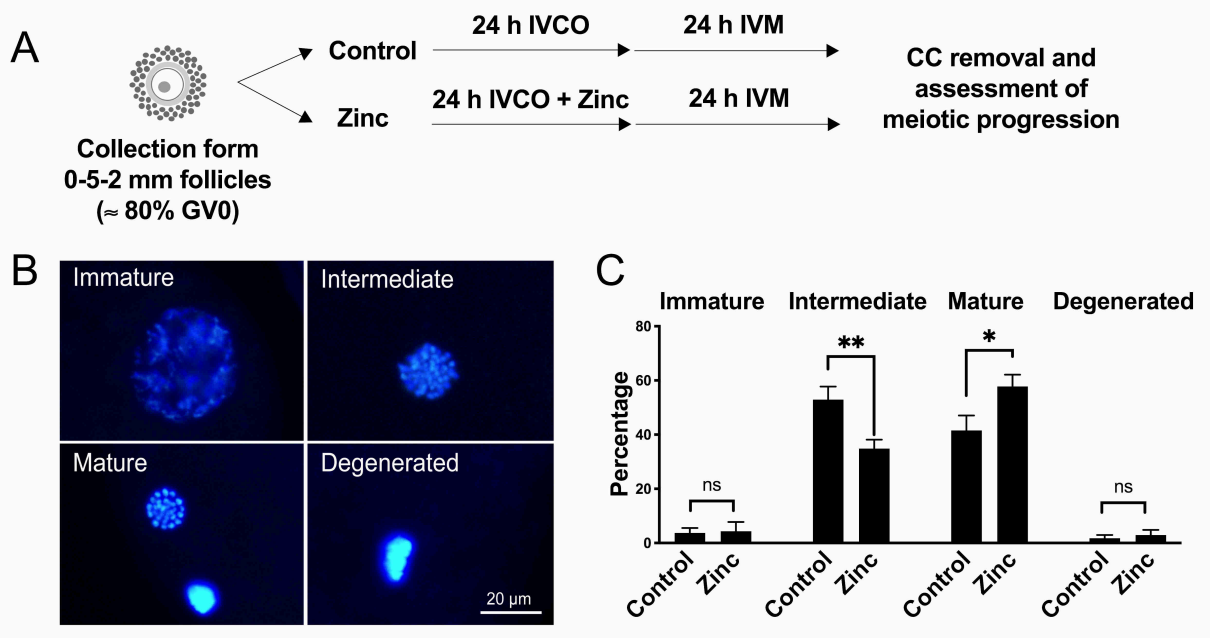

Figure 2: Effect of zinc supplementation during IVCO on meiotic competence acquisition

(**A**) Schematic representation of the experimental design (**B**) Representative epifluorescent images showing immature (GV), intermediate (MI), Mature (MII, polar view and first polar body) and Degenerated oocytes as assessed by DNA staining with DAPI (**C**) Graphs showing the percentage of immature, intermediate, mature and degenerated oocytes in the Control (IVCO in the absence of zinc followed by standard IVM) and zinc (IVCO in the presence of zinc followed by standard IVM) groups. Data were analyzed by Mann-Whithney Test. Values are means ± SEM (n=6). * and ** indicates significant differences between groups (*P<0.05; ** P<0.01). A total of 98 and 102 oocytes were analyzed for Control and zinc groups, respectively in three independent experiments with two technical replicates each.

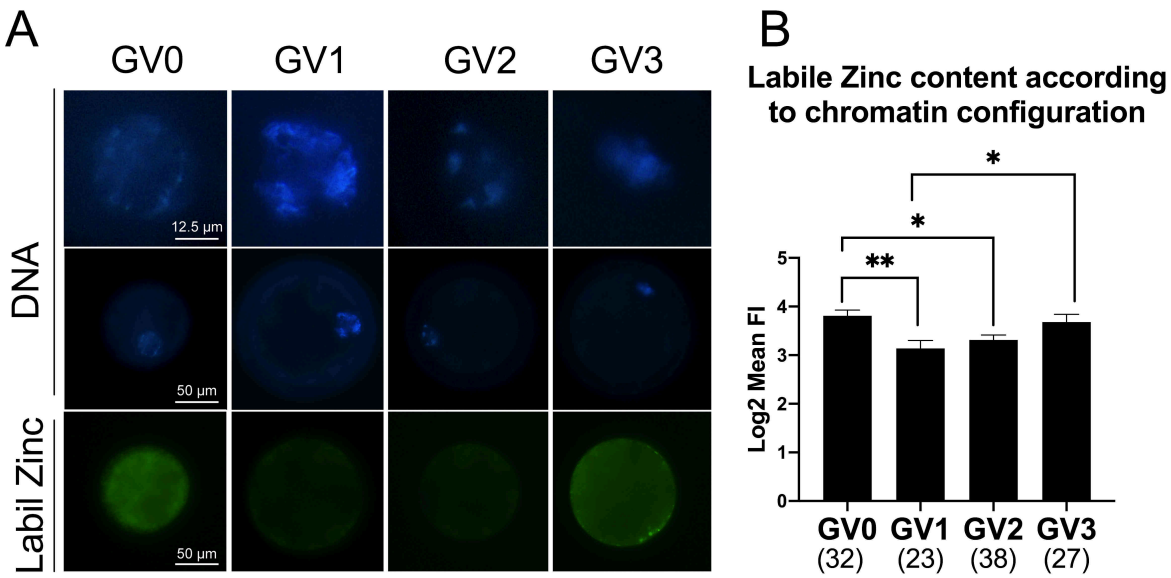

Figure 3: Relationship between large-scale chromatin configuration of the oocyte and labile zinc content

(A) Representative images showing chromatin staining by Hoechst33342 (upper and middle panels) and Labile zinc staining by Fluo Zin (Lower panel) in oocytes with GV0, GV1, GV2 and GV3 chromatin configuration. All Images were captured at the GV focal plane **(B)** Graph showing quantification of labile zinc content as assessed by Fluo Zin loading ad fluorescent image analysis in growing oocytes collected from small antral follicle with a GV0 chromatin configuration, and fully-grown oocytes collected from middle antral follicle with GV1, GV2 and GV3 chromatin configuration as assessed by Hoechst 33342 staining. Total numbers of oocytes analyzed are shown in brackets. Data were pooled together and analyzed by 1-way ANOVA followed by Tukey's multiple comparison test. Values are means ± SEM. * and ** indicate significant differences between groups (*P<0.05; **P<0.01).

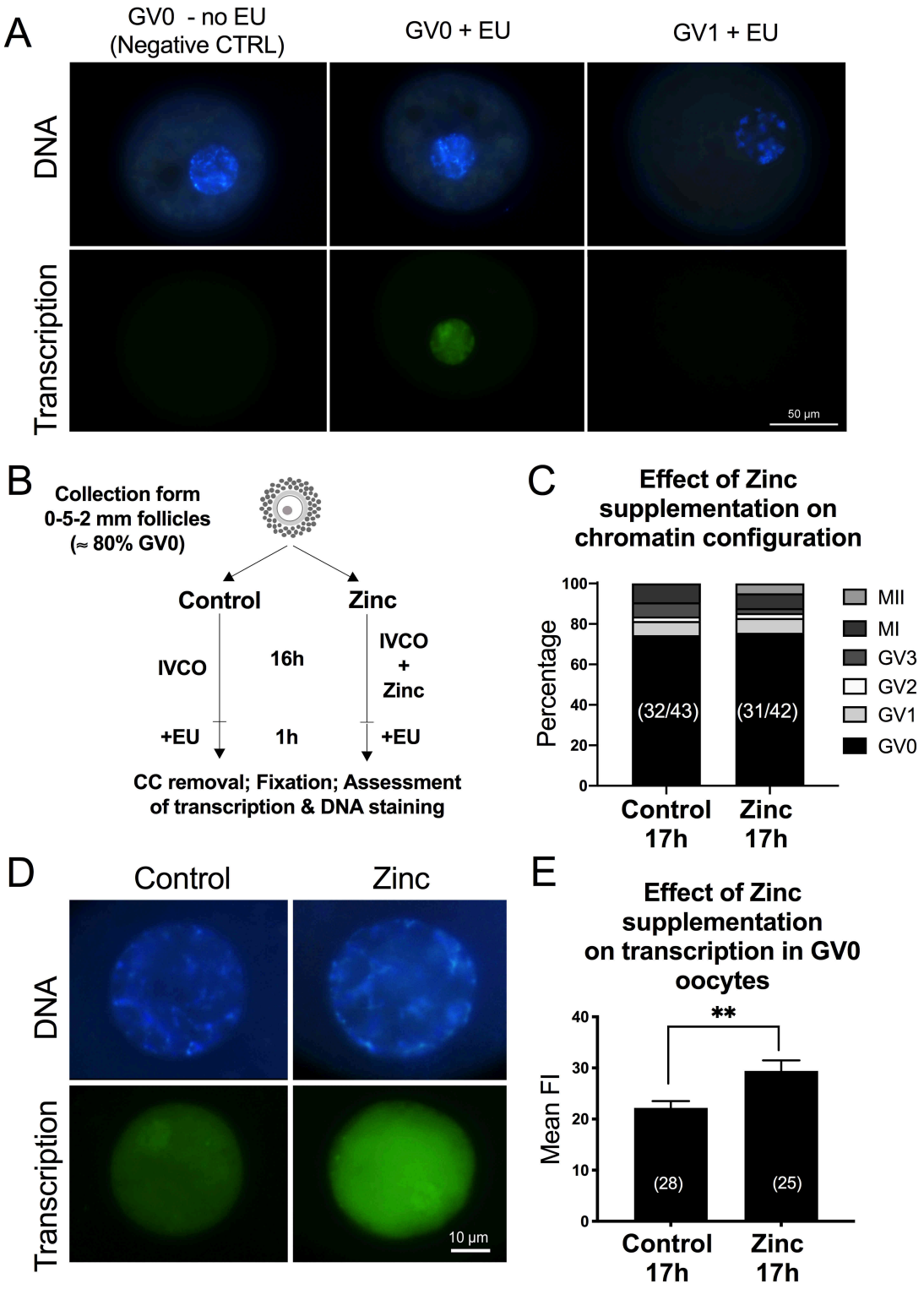

Figure 4: Effect of zinc supplementation during IVCO on global transcriptional activity in GV0 oocytes

(**A**) Representative images showing chromatin staining by DAPI (upper panel) and EU incorporation (lower panel) in GV0 oocytes collected from small antral follicles in the absence (Negative CTRL, left panel) and presence of EU (positive CTRL, middle panel), as well as in a fully-grown oocyte collected from middle antral follicle with a GV1 chromatin configuration (right panel). Note that a positive signal is detected only in GV0

oocytes in the presence of EU. (**B**) Schematic representation of the experimental design (**C**) Graph showing the effect of zinc supplementation during 17h of culture on chromatin configuration and meiotic progression. Total numbers of oocytes analyzed in two independent experiments are indicated in the graph. Note that no differences were observed (**D**) Representative images showing chromatin staining by DAPI (upper panel) and transcription (lower panel) in GV0 oocytes after culture for 17 h under control IVCO condition or in the presence of zinc (**E**) Graph showing quantification of transcriptional activity as assessed by EU incorporation into nascent RNA and fluorescent image analysis in GV0 oocytes cultured in IVCO medium in the absence or presence of zinc. Data were analyzed by unpaired t-test; total number of oocytes analyzed are indicated in parentheses. Values are means ± SEM. ** indicate significant differences between groups (**P<0.01).

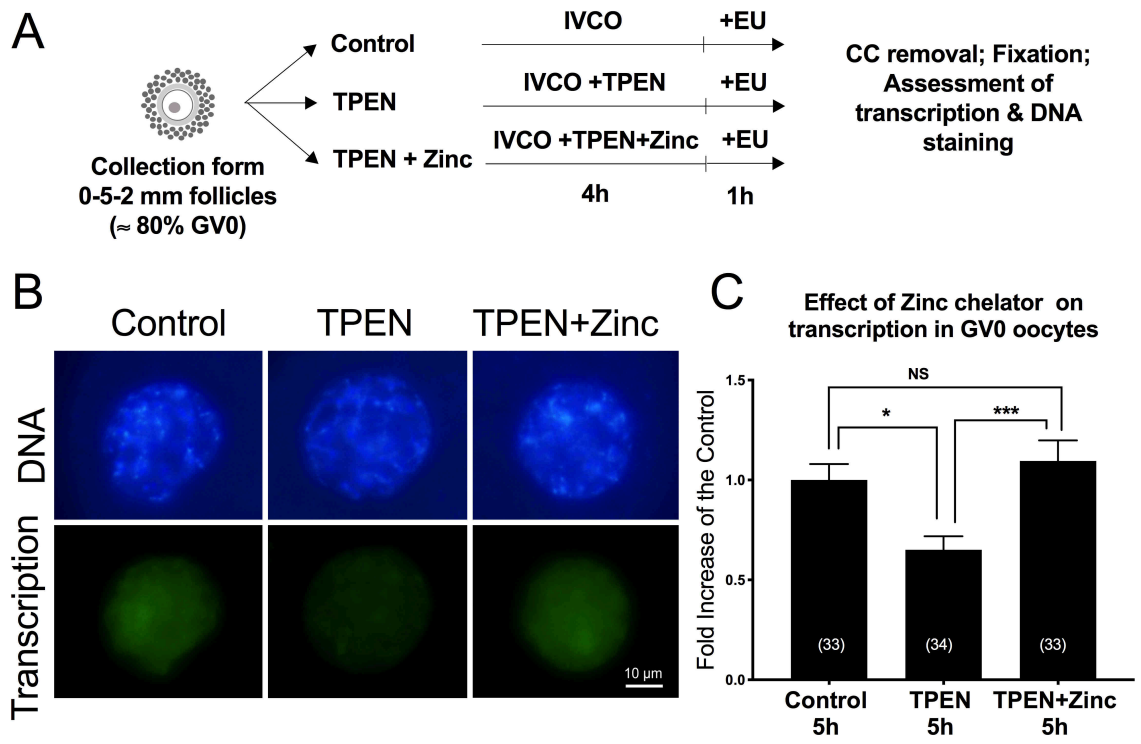

Figure 5: Effect of zinc chelation during 5h IVCO on global transcriptional activity in GV0 oocytes

(**A**) Schematic representation of the experimental design (**B**) Representative images of showing chromatin staining by DAPI (upper panel) and transcription (lower panel) in GV0 oocytes after culture for 5 h under control IVCO condition, in the presence of the zinc chelator TPEN or in the presence of TPEN + zinc (**B**) Graph showing quantification of transcriptional activity in GV0 oocytes cultured in IVCO medium for 5h (CTRL) and in IVCO medium supplemented by TPEN or TPEN + zinc. Data were analyzed by 1 way-ANOVA followed by Tukey's multiple comparison test; total number of oocytes analyzed in three independent experiments are indicated in parentheses. Values are means ± SEM. * and ** indicate significant differences between groups (*P<0.05; **P<0.01).

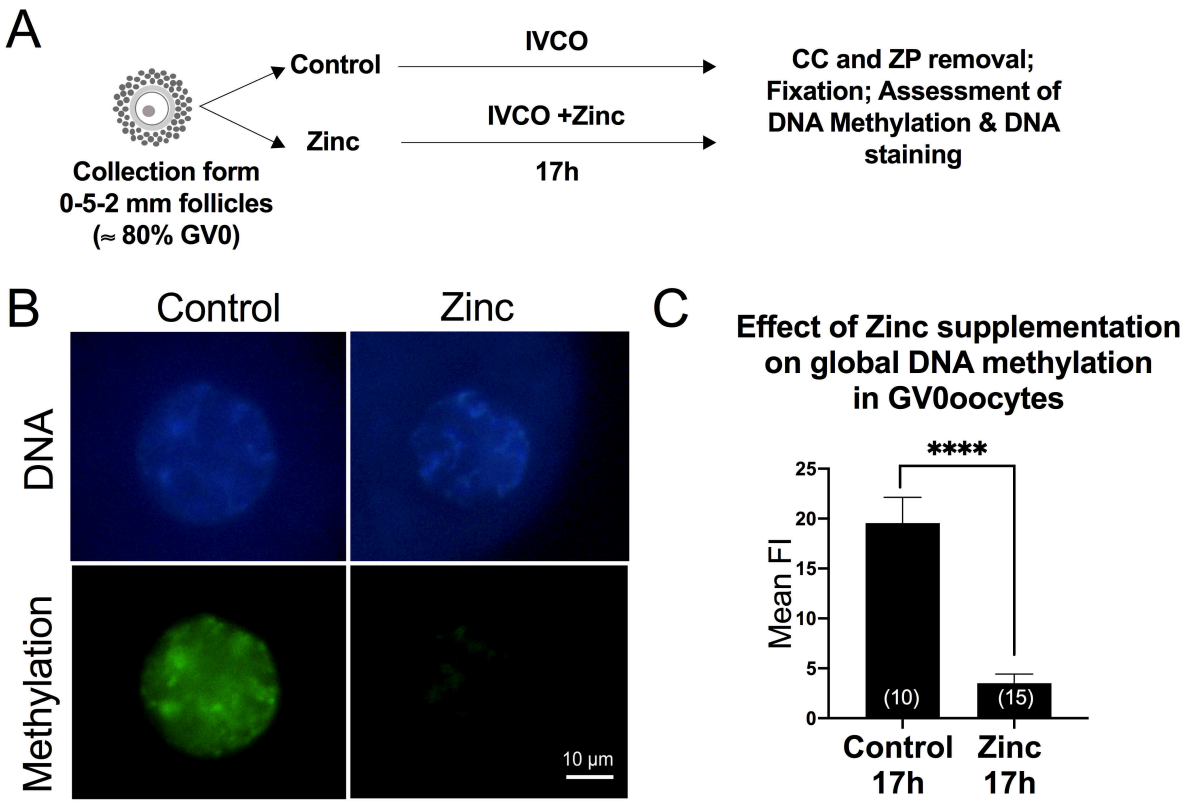

Figure 6: Effect of zinc supplementation during IVCO on global DNA methylation in GV0 oocytes

(**A**) Schematic representation of the experimental groups. (**B**) Representative images showing chromatin staining by DAPI (upper panel) and global DNA methylation (lower panel) in GV0 oocytes after culture in IVCO medium in the Control (IVCO medium) and Zinc (IVCO medium in the presence of zinc groups. (**C**) Graph showing quantification of global DNA methylation as assessed by indirect immunofluorescence and image analysis in GV0 oocytes cultured in IVCO medium in the absence or presence of zinc. Data were analyzed by Mann-Whitney; total number of oocytes analyzed in two independent experiments are indicated in parentheses. Values are means ± SEM. **** indicate significant differences between groups ($P<0.0001$).

Supplemental Fiure 1: FluoZin 3 AM validation

Cumulus oocytes complexes (COC) were collected from middle antral follicles. COCs were loaded with FluoZin™3-AM for 30 minutes as described in the material and methods section. Fluorescent intensity was assessed as described in the method section soon after removal of cumulus cells (Control group, CTRL) or after incubation for 5 minutes in the presence of 100 µM TPEN (TPEN group). The graph shows quantification of labile zinc content in the CTRL and TPEN treated groups. Total numbers of oocytes analyzed in three independent experiments are shown in brackets. Data were pooled together and analyzed by 1-way ANOVA followed by unpaired t-tets. Values are means ± SEM. **** indicate significant differences between groups (P<0.0001).